AMERICAN SOCIETY FOR MICROBIOLOGY | mBio®

RESEARCH ARTICLE
Therapeutics and Prevention

Resistance to a Nucleoside Analog Antiviral Drug from More Rapid Extension of Drug-Containing Primers

Han Chen,[a] Jessica L. Lawler,[a]* David J. Filman,[a] James M. Hogle,[a] Donald M. Coen[a]

[a]Department of Biological Chemistry and Molecular Pharmacology, Blavatnik Institute, Harvard Medical School, Boston, Massachusetts, USA

ABSTRACT Nucleoside analogs are mainstays of antiviral therapy. Although resistance to these drugs hinders their use, understanding resistance can illuminate mechanisms of the drugs and their targets. Certain nucleoside analogs, such as ganciclovir (GCV), a leading therapy for human cytomegalovirus (HCMV), contain the equivalent of a 3′-hydoxyl moiety, yet their triphosphates can terminate genome synthesis (nonobligate chain termination). For ganciclovir, chain termination is delayed until incorporation of the subsequent nucleotide, after which viral polymerase idling (repeated addition and removal of incorporated nucleotides) prevents extension. Here, we investigated how an alanine-to-glycine substitution at residue 987 (A987G), in conserved motif V in the thumb subdomain of the catalytic subunit (Pol) of HCMV DNA polymerase, affects polymerase function to overcome delayed chain termination and confer ganciclovir resistance. Steady-state enzyme kinetic studies revealed no effects of this substitution on incorporation of ganciclovir-triphosphate into DNA that could explain resistance. We also found no effects of the substitution on Pol's exonuclease activity, and the mutant enzyme still exhibited idling after incorporation of GCV and the subsequent nucleotide. However, despite extending normal DNA primers similarly to wild-type enzyme, A987G Pol more rapidly extended ganciclovir-containing DNA primers, thereby overcoming chain termination. The mutant Pol also more rapidly extended RNA primers, a previously unreported activity for HCMV Pol. Structural analysis of related Pols bound to primer-templates provides a rationale for these results. These studies uncover a new drug resistance mechanism, potentially applicable to other nonobligate chain-terminating nucleoside analogs, and shed light on polymerase functions.

IMPORTANCE While resistance to antiviral drugs can hinder their clinical use, understanding resistance mechanisms can illuminate how these drugs and their targets act. We studied a substitution in the human cytomegalovirus (HCMV) DNA polymerase that confers resistance to a leading anti-HCMV drug, ganciclovir. Ganciclovir is a nucleoside analog that terminates DNA replication after its triphosphate and the subsequent nucleotide are incorporated. We found that the substitution studied here results in an increased rate of extension of drug-containing DNA primers, thereby overcoming termination, which is a new mechanism of drug resistance. The substitution also induces more rapid extension of RNA primers, a function that had not previously been reported for HCMV polymerase. Thus, these results provide a novel resistance mechanism with potential implications for related nucleoside analogs that act against established and emerging viruses, and shed light on DNA polymerase functions.

KEYWORDS DNA replication, antiviral drugs, drug resistance mechanisms, ganciclovir, human cytomegalovirus, nucleoside analogs, polymerases

Nucleoside analogs are mainstays of antiviral therapy and are important for anticancer chemotherapy (1). In general, these compounds are phosphorylated intracellularly into drug triphosphates that compete with natural nucleotides to inhibit

Citation Chen H, Lawler JL, Filman DJ, Hogle JM, Coen DM. 2021. Resistance to a nucleoside analog antiviral drug from more rapid extension of drug-containing primers. mBio 12: e03492-20. https://doi.org/10.1128/mBio.03492-20.

Editor Stephen P. Goff, Columbia University/HHMI

Address correspondence to Han Chen, han_chen@hms.harvard.edu, or Donald M. Coen, don_coen@hms.harvard.edu.

* Present address: Jessica L. Lawler, Wiley, Medford, Massachusetts, USA.

This article is a direct contribution from Donald M. Coen, a Fellow of the American Academy of Microbiology, who arranged for and secured reviews by Nell Lurain, Rush University Medical Center, and Fred Homa, University of Pittsburgh School of Medicine.

This work is dedicated to the memory of our cherished collaborator, G. Peter Beardsley.

Received 15 December 2020
Accepted 22 December 2020
Published 9 February 2021

polymerases and/or are incorporated into genomes where they often serve as chain terminators. Resistance to these drugs can limit their effectiveness in the clinic. Understanding resistance mechanisms can shed light on biochemical and biological mechanisms of the drugs, their targets, and the organisms encoding those targets.

The DNA polymerases of herpesviruses are prototypes for family B DNA polymerases, including human DNA polymerases α, δ, and ε, and are also targets of leading drugs for treating herpesvirus infections. The herpesvirus human cytomegalovirus (HCMV) is a common opportunistic pathogen that can cause significant morbidity and mortality, particularly in immunocompromised patients and newborns (2). First-line therapies against HCMV include the nucleoside analog ganciclovir (GCV) and its prodrug, valganciclovir (3). Additionally, ganciclovir in combination with gene delivery of an enzyme that phosphorylates it has been explored as a cancer therapy (4) and as a suicide system to eliminate harmful stem cells following their transplantation (5).

GCV is converted to its triphosphate (GCV-TP), which serves as both a competitive inhibitor and a substrate for the targeted DNA polymerase (6–8). However, unlike a number of nucleoside analogs, GCV is not an obligate chain terminator due to the equivalent of a 3′ hydroxyl group in its sugar moiety. Instead, HCMV DNA polymerase (like other family B DNA polymerases) terminates DNA synthesis after incorporating GCV and the next incorporated (N + 1) nucleotide (6, 9–11) (delayed, nonobligate chain termination).

Prolonged use of GCV can lead to selection for resistance mutations in the gene encoding the catalytic subunit (Pol) of HCMV DNA polymerase that are often associated with treatment failures (12). About half of these GCV resistance (GCV^r) mutations affect residues in or near motifs conserved among 3′–5′ exonuclease (Exo) domains (13). At least three of these mutations impair Exo activity, thereby overcoming chain termination at the N + 1 position by eliminating idling (repeated incorporation of the N + 2 nucleotide followed by its rapid removal), resulting in continued DNA synthesis after incorporation of GCV and the N + 1 nucleotide (14). Moreover, once the N + 1 nucleotide is incorporated, it is not detectably excised, even by wild-type (WT) Pol (14). Thus, studies of Exo mutant HCMV Pols helped elucidate how GCV-TP induces delayed, nonobligate chain termination.

This unusual drug resistance mechanism for GCV^r Exo mutants inspired us to investigate examples of GCV^r mutations that affect the polymerase domain of HCMV Pol (13), which, like other family B DNA polymerases, contains finger, palm, and thumb subdomains. One GCV^r mutation, A987G, which confers ~5-fold resistance to GCV, alters highly conserved region V, which lies within the thumb subdomain of HCMV Pol based on the structure of the closely related herpes simplex virus 1 (HSV-1) Pol (15). This substitution, which was found in the first reported GCV^r mutant (16, 17), has also frequently been detected in clinical isolates associated with treatment failures in transplant recipients (18–20). Structures of family B polymerases bound to DNA primer-templates show that residues in conserved region V directly contact the backbone of the DNA primer (21–23), but functional studies of the effects of mutations in this region have been limited (24). Thus, studying the mechanism of GCV^r conferred by the HCMV A987G substitution may inform our understanding of polymerases across all three domains of life.

Interestingly, whether herpesvirus Pols can utilize RNA primers, which are crucial for initiation of DNA synthesis and for lagging-strand synthesis, has been controversial (25–27). To our knowledge, no one has examined utilization of RNA primers by HCMV DNA polymerase.

Our initial hypothesis was that the A987G substitution would cause GCV^r by altering binding or incorporation of GCV-TP into primer-template, much as the acyclovir resistance (ACV^r) N961K substitution in region V of HSV-1 Pol decreases both binding and incorporation of ACV-TP (28). Alternative hypotheses for resistance mechanisms included increased excision of incorporated GCV, similar to substitutions in the bacteriophage Φ29 DNA polymerase active site that have been reported to induce higher

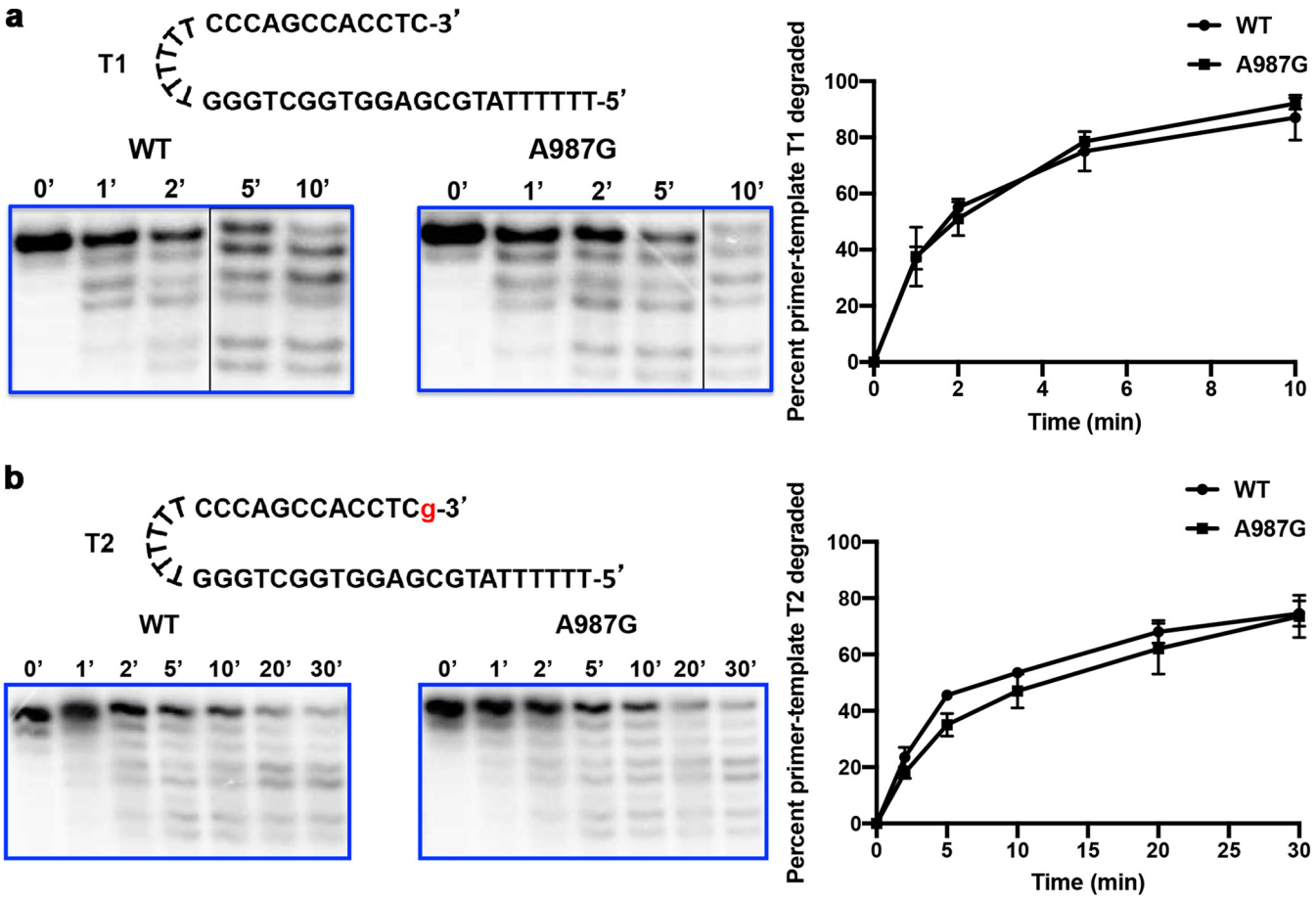

FIG 1 Similar degradation of dC-terminated primer-template T1 (a) and GCV-terminated primer-template T2 (b) by WT Pol and A987G Pol. 5′-Radiolabeled primer-template T1 or T2 (sequences above the gel images in panels a and b, respectively; g, GCV) was incubated with WT Pol or A987G Pol (indicated above each gel image) in the presence of UL44 and absence of dNTPs at 37°C for the times indicated above each lane in the gel image. The reactions were analyzed by polyacrylamide gel electrophoresis and autoradiography (gel images in panels a and b) as well as a phosphorimager to quantify the percentage of starting primer-template that was degraded (graphs on right of panels a and b). Error bars indicate standard errors of the means (SEM) from two independent replicates. The thin black vertical lines in the gel images in panel a indicate where empty lanes were removed from the original images.

Exo activity than that of the WT (29), and continued DNA synthesis after incorporating GCV and one additional nucleotide, akin to the DNA extension pattern induced by HCMV Exo mutations (14). Our investigations here distinguish among these hypotheses, revealing a new mechanism of drug resistance, and notably, uncover unexpected results regarding the extension of RNA primers by HCMV Pol.

RESULTS

No meaningful effects at the initial step of GCV incorporation. To determine how the Pol substitution A987G confers GCV resistance, we purified WT HCMV Pol and A987G Pol as glutathione *S*-transferase (GST) fusion proteins from recombinant baculovirus-infected insect cells (14). We first tested whether the mutant enzyme is impaired for its ability to bind and incorporate GCV-TP into DNA. We used a steady-state enzyme kinetics approach under Michaelis-Menten conditions (11, 14, 28, 30) (see Fig. S1 in the supplemental material), measuring apparent K_m and k_{cat} values for incorporation of GCV-TP or dGTP into a 40-mer hairpin primer-template T1 (Fig. 1a), radiolabeled on its 5′ end. We also measured apparent K_i values for GCV-TP inhibition of dGTP incorporation using the same primer-template. UL44, the presumptive HCMV polymerase processivity subunit, was omitted to reduce the contribution of dissociation of polymerase from primer-template to the rate of incorporation.

A987G Pol exhibited apparent K_m values for GCV-TP and dGTP, an apparent k_{cat}

TABLE 1 Apparent kinetic constants[a] for incorporation of dGTP and GCV-TP into primer-template T1 by WT Pol and A987G Pol

	GCV-TP			dGTP	
Name	K_m, μM	k_{cat}, min^{-1}	K_i, μM	K_m, μM	k_{cat}, min^{-1}
WT[b]	5.5 ± 1.2	1.7 ± 0.17	3.4 ± 1.4	0.44 ± 0.05	22 ± 0.70
987G	5.8 ± 1.5	2.2 ± 0.18	5.1 ± 1.3	0.34 ± 0.09	11 ± 0.67

[a]Values ± SEM generated from two independent replicates. Apparent K_m values were determined by fitting data points to the Michaelis-Menten equation using GraphPad Prism (version 6). Apparent k_{cat} values were determined by dividing apparent V_{max} values by the enzyme concentrations. Apparent K_i values were determined by fitting data to a competitive inhibition model using GraphPad Prism (version 6).
[b]Apparent kinetic constants for the WT are from references 14 and 59; A987G was analyzed in the same experiments but not reported at the time.

value for incorporation of GCV-TP, and an apparent K_i for GCV-TP inhibition of dGTP incorporation that were well within 2-fold of those of WT Pol (Table 1). The mutant Pol did exhibit a 2-fold lower apparent k_{cat} value for incorporation of dGTP relative to WT Pol, but that would not explain its GCV resistance, as, if anything, reduced incorporation of dGTP would be expected to increase GCV susceptibility. Thus, we found no evidence that the A987G substitution confers GCV resistance at the step of incorporation of GCV-TP into primer-template.

No increased excision of incorporated GCV. We next investigated whether the A987G substitution increases the ability of Pol's 3′–5′ Exo to excise incorporated GCV. Incubation of WT Pol or A987G Pol with either radiolabeled synthetic primer-template T1 terminated with dC (Fig. 1a) or primer-template T2 terminated with GCV (Fig. 1b) in the absence of deoxynucleoside triphosphates (dNTPs) and the presence of the HCMV DNA polymerase accessory subunit UL44 resulted in very similar rates of degradation by both enzymes (Fig. 1). We conclude that the Pol mutation A987G does not confer resistance by increasing excision of incorporated GCV.

Continued extension after incorporation of GCV-TP. We then asked if the A987G substitution allows HCMV Pol to continue DNA synthesis after incorporation of GCV-TP and the subsequent nucleotide at the N + 1 position, akin to the DNA extension pattern induced by GCV^r Exo mutations (14). To this end, WT Pol, A987G Pol, and, as a positive control, the HCMV Exo mutant F412V that we characterized previously (14) were each incubated with radiolabeled primer-template T1 (Fig. 1a) in the presence of UL44, GCV-TP, dATP, dCTP, and dTTP (dGTP was omitted). As expected, WT Pol efficiently terminated DNA synthesis after incorporating GCV-TP plus one additional nucleotide (in this case, dCTP) (Fig. 2). Consistent with our previous study (14), Exo mutant F412V was able to continue DNA synthesis to the end of the template after incorporating GCV-TP and dCTP, despite ~50% termination at the N + 1 position (Fig. 2). Interestingly, after A987G Pol incorporated GCV-TP into primer-template T1, there was less termination following incorporation of dCTP into the N + 1 position, with most DNA synthesis continuing to the end of the template, particularly at the higher enzyme concentration (Fig. 2). Similar to previous results with Exo-deficient mutants (14), the full-length products generated by A987G Pol were not the result of misincorporation of dATP, dCTP, or dTTP opposite dC in the template, because there was no DNA extension in the absence of GCV-TP, and full-length products synthesized in the presence of GCV-TP exhibited altered electrophoretic mobility relative to those synthesized in the presence of dGTP (Fig. S2). These results support the hypothesis that the A987G substitution confers resistance by permitting the enzyme to continue DNA synthesis following incorporation of GCV plus the next nucleotide.

A987G Pol still idles. Following incorporation of GCV-TP and the subsequent nucleotide, WT Pol repeatedly adds the incoming dNTP and then rapidly removes it to generate dNMP (idling), thereby terminating extension at the N + 1 position (14). In contrast, Exo mutants exhibit little or no idling, so they overcome chain termination and continue synthesis (14). To test whether A987G Pol eliminates idling, we incubated WT Pol, A987G Pol, and, as a control, Exo mutant F412V Pol with a synthetic primer-

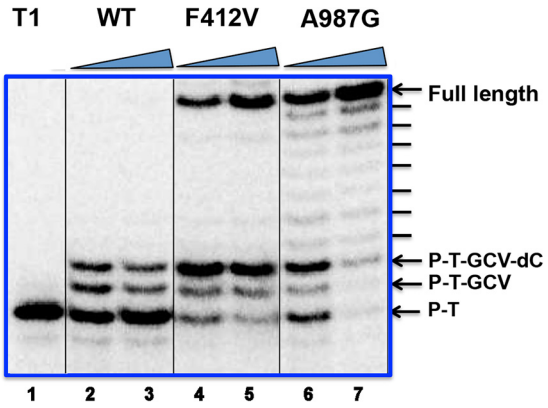

FIG 2 Limited DNA extension by WT Pol and full-length extension by A987G Pol following GCV-TP incorporation. Radiolabeled primer-template T1 (Fig. 1a) was incubated with GCV-TP, dATP, dCTP, dTTP, and each of the indicated Pols (7.2 nM for lanes 2, 4, and 6; 8.4 nM for lanes 3, 5, and 7) in the presence of UL44 at 37°C for 30 min, and the products were analyzed alongside untreated T1 by polyacrylamide gel electrophoresis and autoradiography. Leftmost lane, untreated radiolabeled T1. For the remaining lanes, enzymes used are indicated at the top of the panel, and the wedge indicates increasing concentrations of each enzyme. The arrows to the right of the panel indicate the major species observed. P-T, unmodified primer-template T1; P-T-GCV, T1 with GCV added; P-T-GCV-dC, T1 with GCV and dC added as well as full-length product. The dashes to the right of the panel indicate minor products. The thin black vertical lines in the gel image indicate where lanes containing reactions performed at lower polymerase concentrations and/or using Exo-deficient mutants other than F412V were removed to reduce the size of the image.

template T3 terminated with GCV plus dC (Fig. 3a) and assayed for generation of labeled dAMP in the presence of [α-^{32}P]dATP using thin-layer chromatography (TLC). In this assay, both WT Pol and A987G Pol converted similar amounts of dATP to dAMP (both ~10%), and substantially more than F412V Pol converted (~0.7%) (Fig. 3b), indicating that the A987G substitution did not eliminate idling. To follow up this finding, we examined whether WT Pol and A987G Pol could efficiently degrade a radiolabeled primer-template, T4 (Fig. 3c), terminated with GCV plus dC and, in the N + 2 position, dA. Consistent with the results of the idling assay in the absence of dNTPs, both WT (as previously observed [14]) and A987G Pols rapidly degraded primer-template T4 at indistinguishable rates (Fig. 3d), generating N + 1 primer-template without further degradation (Fig. 3d). As before (14), F412V Pol was substantially impaired for degrading the N + 2 primer-template T4 (Fig. S3). Taken together, these results indicate that the A987G substitution does not eliminate idling, and that A987G Pol and the Exo mutant F412V Pol use different mechanisms to enable continued DNA synthesis following incorporation of GCV-TP into DNA.

More rapid extension of GCV-containing N + 1 and N + 2 primers. We hypothesized that the A987G substitution increases the enzyme's rate of extension of primers containing GCV, allowing the polymerase to overcome GCV-induced chain termination and continue DNA synthesis. To test this hypothesis, we first analyzed the rates of dCTP incorporation by WT and mutant Pols on the N primer-template T2 terminated with GCV (Fig. 1b). The incubation of radiolabeled primer-template T2 with WT Pol or A987G Pol in the presence of UL44 and dCTP (no other dNTPs) resulted in similar rates of formation of N + 1 product (Fig. 4a and Table 2). Next, we examined dATP incorporation on the N + 1 primer-template T3 terminated with GCV plus dC (Fig. 3a) to assess incorporation of the second nucleotide (N + 2). A987G Pol (with UL44) extended the N + 1 primer-template more rapidly than did WT (Fig. 4b and Table 2). Finally, when we incubated the enzymes with radiolabeled N + 2 primer-template T4 terminated with GCV-dC-dA (Fig. 3c) in the presence of UL44 and dTTP, A987G Pol again generated N + 3 products more rapidly than did WT Pol (Fig. 4c and Table 2; extension plateaued after 20 s of incubation, accompanied by rapid Exo degradation of the starting N + 2 primer-template and N + 3 products).

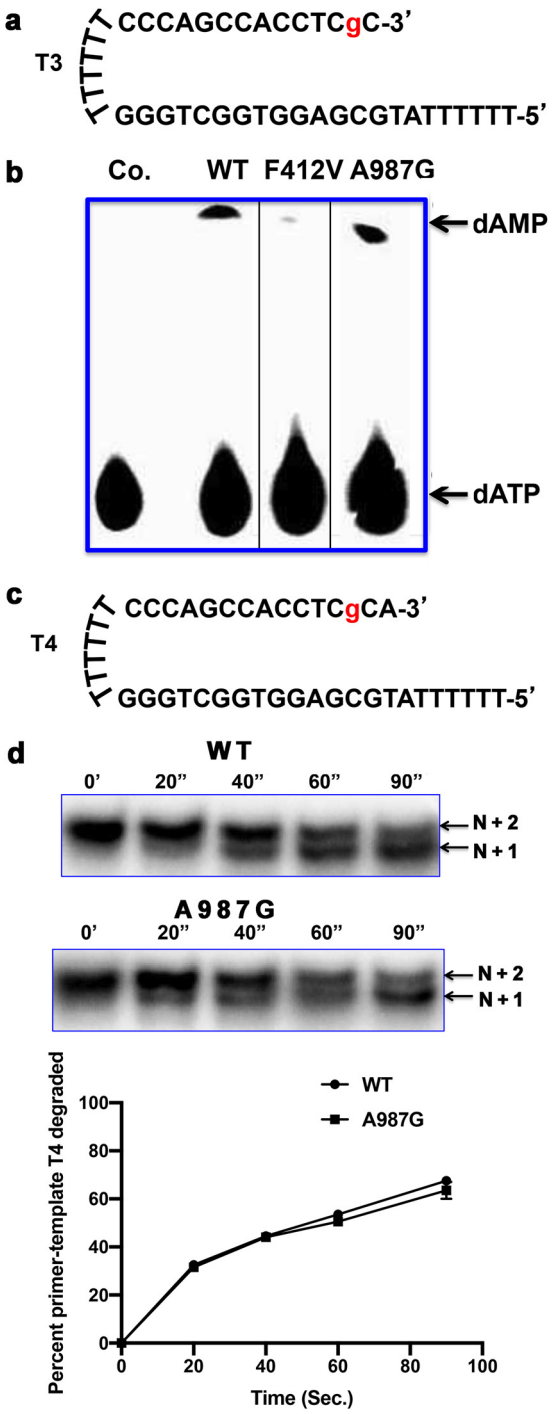

FIG 3 Similar idling and exonuclease activity of WT Pol and A987G Pol on primer-templates containing internally incorporated GCV. (a) The sequence of N + 1 primer-template T3; g, GCV. (b) T3 was incubated with [α-^{32}P]-labeled dATP either in the absence of enzyme (Co.) or using the enzymes indicated at the top of the panel in the presence of UL44 at 37°C for 10 min, and the products were analyzed by TLC and autoradiography. The positions of dATP and dAMP were determined by visualizing unlabeled standards under UV light and are indicated by arrows to the right of the panel. The thin black vertical lines indicate where lanes from reactions with Exo-deficient mutants other than F412V were removed from the image to reduce its size. (c) The sequence of N + 2 primer-template T4; g, GCV. (d) T4 was incubated with WT Pol and A987G Pol in the presence of UL44 and absence of dNTPs for the times indicated above each panel. The products were analyzed by polyacrylamide gel electrophoresis and autoradiography (top) or a phosphorimager (bottom), which was used to quantify the percentage of starting primer-template that was degraded. Error bars indicate SEM from two independent replicates. The arrows to the right of the autoradiogram indicate the positions of T4 (N + 2) and the product (N + 1) generated by removal of a single nucleotide from T4.

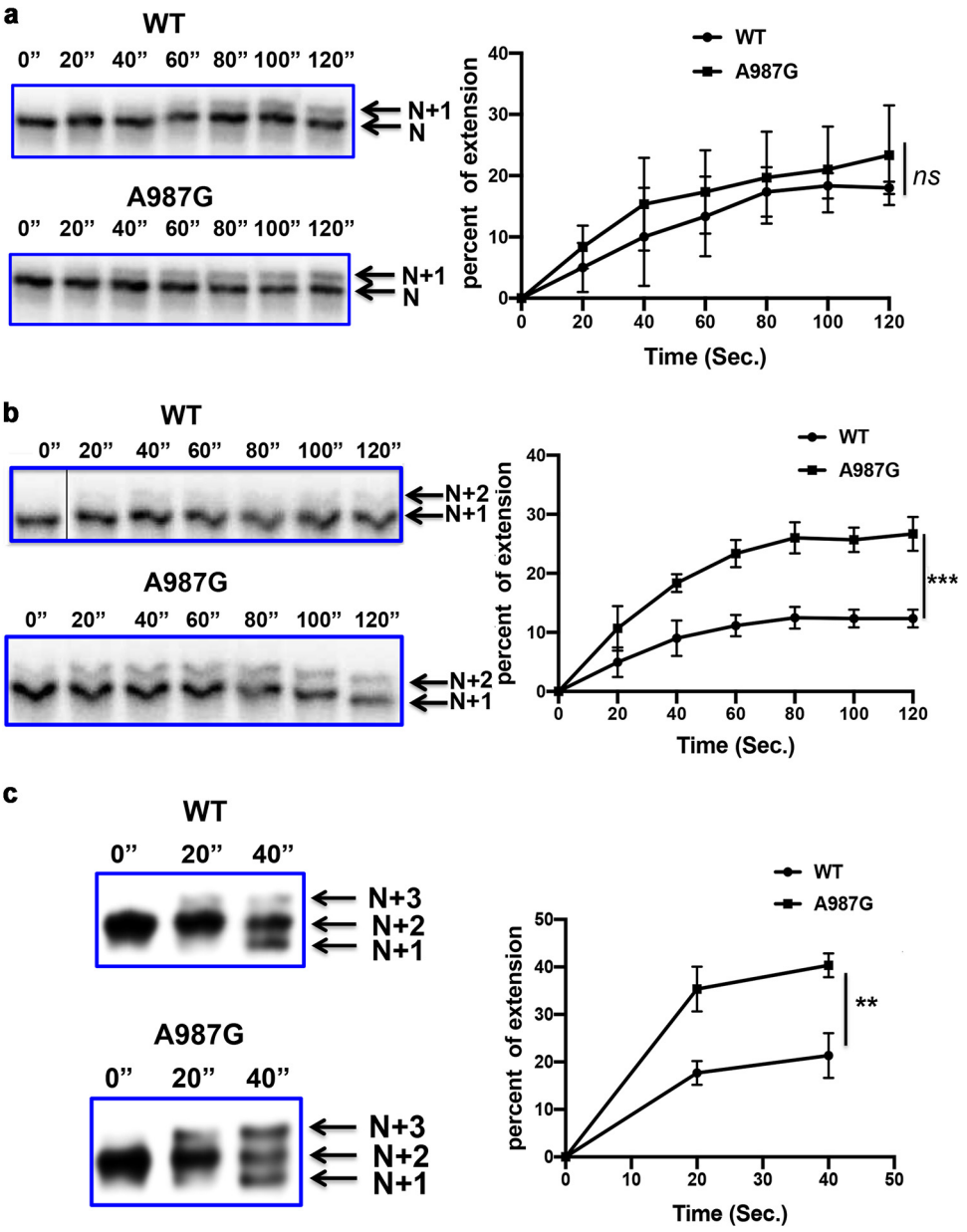

FIG 4 Single-nucleotide incorporation by WT Pol and A987G Pol on GCV-containing primer-templates. Radiolabeled primer-template T2 terminating with GCV (Fig. 1b) plus dCTP (a), N + 1 primer-template T3 (Fig. 3a) plus dATP (b), or N + 2 primer-template T4 (Fig. 3c) plus dTTP (c) was incubated with WT Pol or A987G Pol in the presence of UL44 at 37°C for the times indicated above each lane of the gel images. The products were analyzed by polyacrylamide gel electrophoresis and autoradiography. The positions of the starting primer-template and each product are indicated by arrows (right side of the gel image in each panel). The thin vertical black line in the image in panel b indicates where an empty lane was removed from the original image. The percentages of products that were larger (by one nucleotide) than their corresponding primer-templates in each gel lane were quantified using a phosphorimager and are plotted against incubation time (in panel c, only the products generated within 40 s were analyzed due to the rapid degradation of the T4 primer-template). Error bars shown in the plot of each panel indicate standard deviations based on three independent experiments. *P* values were obtained using repeated-measures two-way analysis of variance in GraphPad Prism 8. *ns*, not significant; **, $P = 0.0014$; ***, $P = 0.0029$.

We compared extension and degradation rates on each primer-template by WT Pol and A987G Pol (Table 2). (Because the rates of extension and degradation varied among different primer-templates, different concentrations of Pol were used [Table 2] to permit sufficient detection of product while achieving linear rates). WT Pol and

TABLE 2 Comparison of the rates[a] for extension and degradation of each primer-template by WT Pol and A987G Pol

			Extension[b] (nM/min)		Degradation[b] (nM/min)	
P-T	Nucleoside	Enzyme (nM)	WT	A987G	WT	A987G
T1	GCV-TP	30	48 ± 2	53 ± 3	30 ± 5	31 ± 3
T2 (N)	dCTP	10	30 ± 5	38 ± 5	20 ± 4	15 ± 5
T3 (N + 1)	dATP	10	6 ± 1	14 ± 2	ND[c]	ND[c]
T4 (N + 2)	dTTP	30	36 ± 1	72 ± 4	59 ± 3	57 ± 2

[a]The extension rates for incorporation of GCV-TP or the relevant dNTP indicated in each row and the degradation rates on each primer-template were determined by plotting the amount of extended or degraded primer-templates versus time. P-T, primer-template.
[b]Errors are SEM generated from two independent replicates.
[c]ND, not detectable.

A987G Pol extended primer-template T1 by incorporating GCV-TP into the N position at similar rates (Table 2, Fig. S4), consistent with their similar apparent k_{cat} values (Table 1). These rates of GCV-TP incorporation were relatively low compared with extension using dGTP (Table 1) and only ~1.7-fold higher than the degradation rates on the same primer-template. On primer-template T2, which contains GCV in the N position, the two enzymes again exhibited similar rates of incorporation of dCTP at the N + 1 position that were just slightly higher than the degradation rates. On primer-template T3, no degradation could be detected (as previously observed [14]). Here, although the rates of extension were low for both enzymes, A987G Pol exhibited an ~2-fold higher extension rate than the WT in incorporating dATP at the N + 2 position. Once incorporated, WT enzyme more rapidly removes that nucleotide than extends it to the N + 3 position, as seen using primer-template T4 (Fig. 4c). In contrast, A987G not only more rapidly generates primer-template terminated at the N + 2 position than does WT but also more rapidly extends it to the N + 3 position, with the rate of extension being ~2-fold greater than that of the WT. Importantly, that rate of extension is greater than the rate of degradation of the N + 2 primer-template (Table 2), permitting DNA synthesis to continue. These analyses support a model for how A987G Pol overcomes GCV-induced chain termination, which we summarize below in Discussion.

Utilization of RNA primers. In the nuclear magnetic resonance (NMR) structure of a 10-bp oligonucleotide containing GCV, the internal GCV moieties induce distortion in the DNA backbone so that it locally resembles A-DNA (31). Given that an RNA primer bound to DNA template results in an A-form duplex (32), we hypothesized that the A987G mutant Pol can extend RNA primers relatively efficiently. To our knowledge, HCMV Pol has not previously been tested for its ability to extend RNA primers.

To test this hypothesis, we used two 5′ fluorescently labeled hairpin primer-templates, here named T5 and T6 (previously designated S1 and S2 [33]), with the same template sequence but with T5 containing a DNA primer (Fig. 5a) and T6 containing the corresponding RNA primer (Fig. 5b). As a control, we initially tested WT HSV-1 Pol using these two primer-templates. Despite reports that HSV-1 Pol extends RNA primers inefficiently (25, 34), we found that it could extend the RNA primer in T6 effectively, converting all primer-template to full-length products, albeit less rapidly than its extension of the DNA primer in T5 (Fig. S5).

We then tested WT Pol and A987G Pol. Both enzymes extended the DNA primer in T5 at similar rates, with nearly half of the primer extended within 30 s (Fig. 5a). Both enzymes also extended the RNA primer in T6 to full-length products (Fig. 5b). In line with our hypothesis, A987G Pol extended RNA primers more efficiently than the WT, with 60% of RNA primer converted to full-length products after 5 min of incubation, while WT Pol only converted 10% of RNA primers to full-length products within the same time (Fig. 5b). The addition of UL44 had little, if any, effect on the ability of the

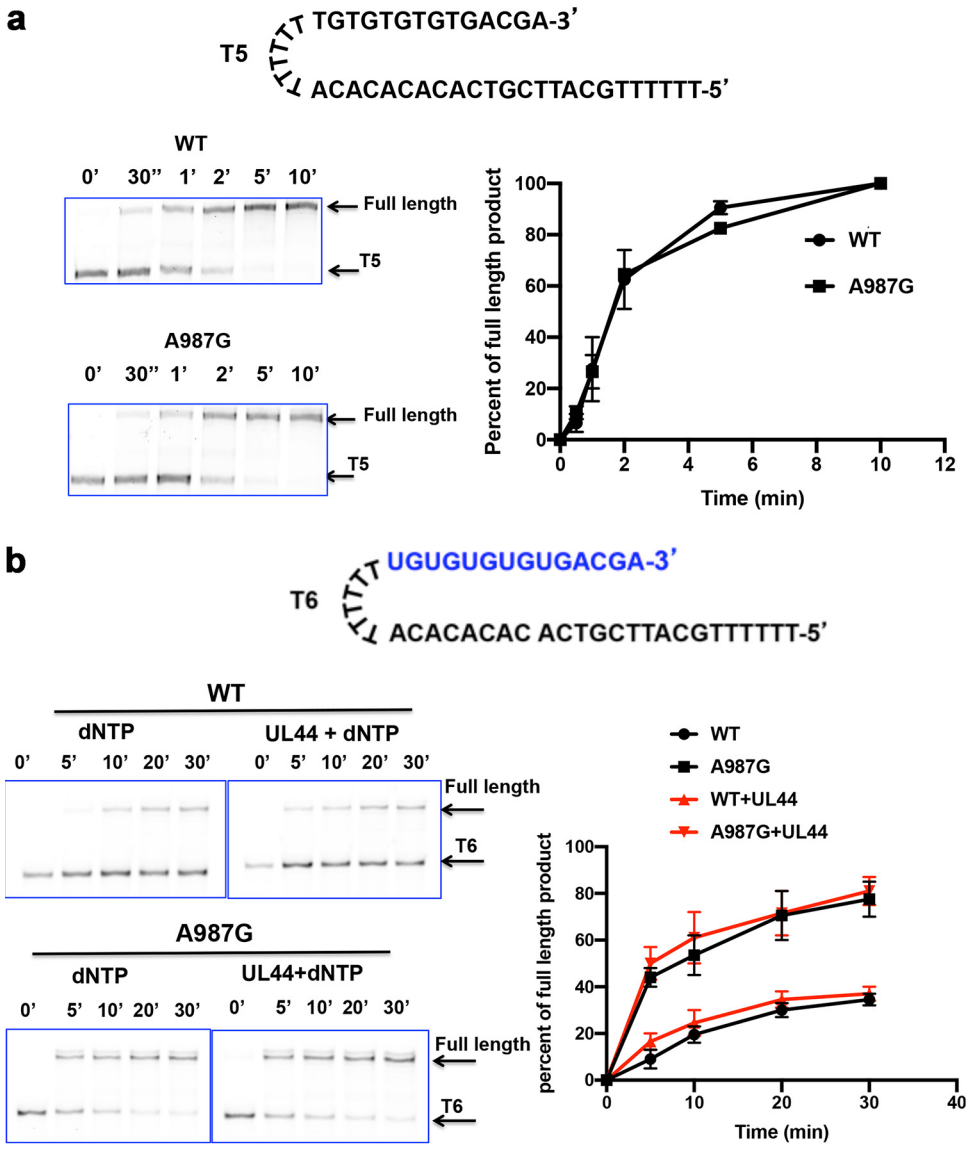

FIG 5 Extension of DNA and RNA primers by WT Pol and A987G Pol. (a, top) The sequence of FAM-labeled DNA primer-template T5. (Left) T5 was incubated with each of the indicated Pols and dNTPs at 37°C for the times indicated on the top of each lane of the gel image. The products were analyzed by polyacrylamide gel electrophoresis and fluorescent imaging. The arrows to the right side of the gel images indicate the positions of full-length products and T5. (Right) The percentages of full-length products were quantified using ImageJ and were plotted against incubation time. Error bars indicate SEM based on two independent replicates. (b, top) The sequence of 6-FAM-labeled primer-template T6; the RNA portion is in blue. T6 was incubated with each of the indicated Pols and dNTPs in the presence or absence of UL44 at 37°C for the times indicated on the top of each lane of the gel image on the left. The full-length DNA products were analyzed, quantified, and plotted against the incubation time on the right as described for panel a. The positions of full-length DNA product and primer-template T6 are indicated by arrows to the right of the gel image, and error bars in the plot indicate SEM from two independent replicates.

enzymes to extend an RNA primer (Fig. 5b). Thus, HCMV Pol can utilize and extend RNA primers, and the A987G mutation increases that activity.

DISCUSSION

Mutations in polymerase genes that confer resistance to nucleoside analogs usually do so by reducing binding and/or incorporation of drug TPs or by increasing excision of incorporated drugs (3). In contrast, HCMV Pol Exo mutants confer resistance to GCV by preventing idling, permitting the extension of GCV-containing primers (14). Here,

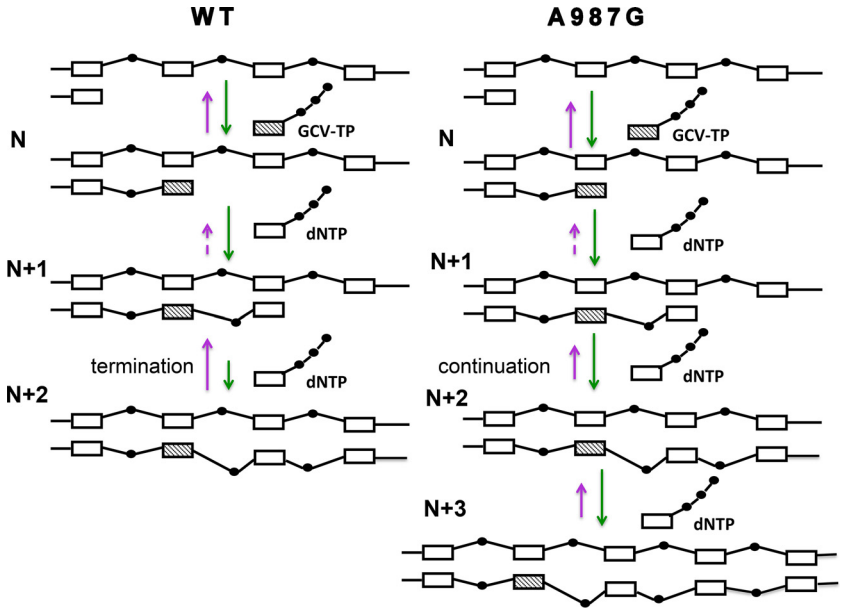

FIG 6 Model for chain termination by WT Pol (left) and chain elongation by A987G Pol (right) after incorporating GCV and one additional nucleotide. Each open box and the black dot that follows in the template strand represented at the top indicate deoxynucleoside monophosphates within DNA. The primer strand grows from left to right and incorporates GCV-TP (hatched box with a line of three black dots) to form the N primer-template and subsequently natural dNTPs (open box with a line of three black dots) at each position (N + 1, N + 2, and N + 3), indicated at the left side of corresponding primer-template. The asymmetric lines connecting GCV and the subsequent two nucleotides at N + 1 and N + 2 indicate the distortion in the sugar-phosphate backbone induced by GCV (57). Turquoise vertical arrows pointing down represent incorporation, and the magenta arrows pointing up represent excision. The relative lengths of turquoise and magenta arrows indicate relative rates for extension and degradation of each primer template. The short dashed magenta lines represent the undetectable degradation of N + 1 primer template. See the text for a discussion.

we found the HCMV Pol mutant A987G, with a substitution in a conserved motif (region V) of the thumb domain, adopts an entirely new mechanism to confer resistance to GCV. As summarized in Fig. 6, like WT enzyme, this mutant can incorporate GCV-TP plus the subsequent nucleotide (N + 1 position). Like WT enzyme, its Exo activity does not detectably degrade this primer-template but idles due to high Exo activity on the N + 2 extension product. However, unlike WT enzyme, A987G Pol can escape idling and thus overcome chain termination at the N + 1 position by extending both the N + 1 and N + 2 drug-containing primer-templates more rapidly than its Exo can degrade them.

The A987G substitution alters conserved region V of family B DNA polymerases, which includes a sequence motif with two basic residues followed by two less conserved residues (R984, K985, T986, and A987 for WT HCMV) (Fig. 7a). There is currently no published structure of a herpesvirus Pol bound to primer-template. To understand the effects of the A987G mutation on Pol's activity to extend GCV-containing DNA primers, we examined the structure of the most closely related family B DNA polymerase that has been solved bound to a DNA primer-template (and an incoming nucleotide): yeast (*Saccharomyces cerevisiae*) DNA polymerase δ (23) (PDB entry 3IAY). In this model, the sequence motif R839, R840, D841, and S842 in region V of the thumb subdomain corresponds to the motif containing residues R984, K985, T986 and A987 in HCMV Pol (Fig. 7b). The two basic residues (yeast R839 and R840) contact the backbone of the primer strand, which is in turn base paired with template (Fig. 7c). The yeast residue corresponding to HCMV A987 (in this case S842) makes no contacts with DNA, but its side chain does help hold these basic residues in place by interacting with a section of alpha helix (C843 to E860) just N-terminal of the basic residues and with a

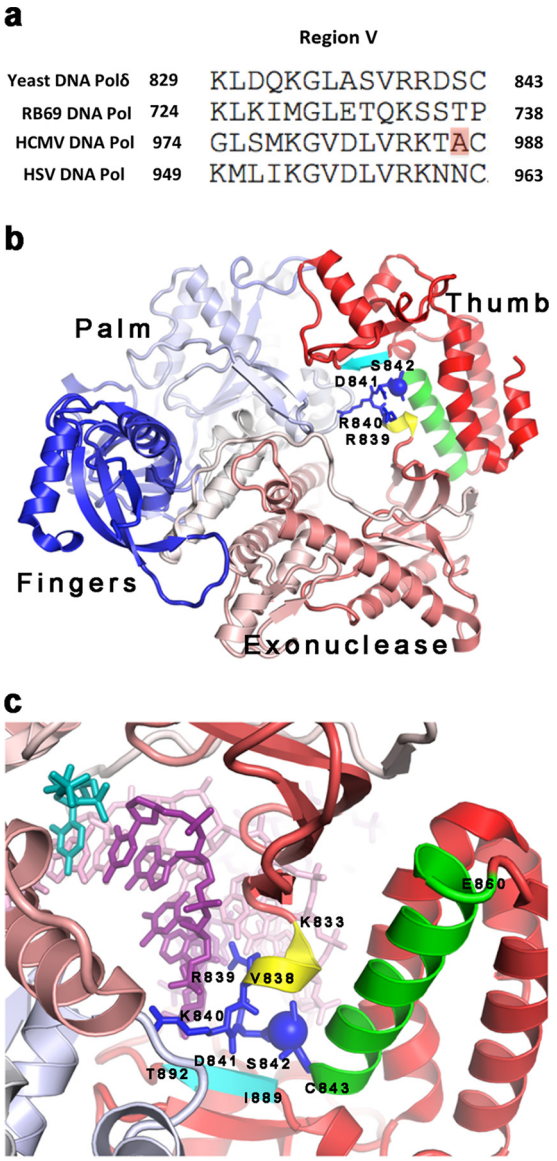

FIG 7 Location and contacts of the residue corresponding to HCMV residue A987 in the polymerase active site of yeast DNA polymerase δ bound to primer-template and dNTP (PDB entry 3IAY). (a) Amino acid sequence alignment of conserved region V of family B DNA polymerases from yeast DNA polymerase δ (Polδ), bacteriophage RB69 DNA Pol, HCMV DNA Pol, and HSV-1 DNA Pol. The position of HCMV Pol residue A987 is highlighted in red. (b) The Pol δ fingers, palm, most of the thumb and exonuclease domains are shown in dark blue, white, red, and light orange, respectively. The conserved RRxx motif (yeast Pol δ R839, R840, D841, S842), corresponding to residues R984, K985, T986, and A987 of HCMV Pol, is shown as a dark blue stick model. S842, corresponding to HCMV Pol reside A987, is highlighted as a dark blue sphere. An adjacent α-helix, β-turn, and β-strand are shown in green, yellow, and cyan, respectively. DNA and the incoming nucleotide in the structure are omitted for clarity. (c) Close-up view of the contacts of residue S842 corresponding to HCMV Pol A987. The blue stick model represents residues 839 to 842 with residue 842 shown as a blue sphere. Residues I889 to T892 in the Pol δ sequence, which form a β-strand, and residues C843 to E860, which form a long α-helix, are colored in cyan and green, respectively. Residues K833 to V838, corresponding to the site of an HCMV deletion that confers drug resistance, form a β-turn and are highlighted in yellow. The DNA primer strand, template strand, and incoming nucleotide dCTP in the structure are in dark purple, pink, and teal, respectively.

nearby beta strand formed by residues I889 to T892 (Fig. 7c; a roughly similar arrangement is found in the structure of another family B polymerase bound to primer-template and incoming nucleotide, the phage RB69 Pol [22]) (Fig. S6a; PDB entry 1IG9). Replacement of this residue with a glycine (G), which is highly flexible and whose side

chain (H) would not interact with other nearby protein segments, would be expected to make the interaction with primer less rigid and, thus, better able to accommodate the changes in the primer backbone due to incorporated GCV (31) or ribonucleoside moieties. The less rigid structure might also account for the slightly lower apparent k_{cat} than that of the WT for dGTP incorporation. We note the possibility that local sequence variations might modulate the distortions induced by incorporated GCV, which in turn could affect how efficiently GCV induces chain termination and how effectively the A987G mutation overcomes such termination.

To understand the lack of effect of the A987G mutation on Exo activity, we also examined the structure of the family B DNA polymerase from phage RB69 bound to primer-template, in this case with primer in the Exo active site (35) (PDB entry 1CLQ). In this structure, the residues corresponding to HCMV Pol R984 and K985, or any other residues expected to be affected by changes in the residue corresponding to HCMV Pol A987, do not interact with primer (Fig. S6b). This would explain why the HCMV A987G substitution does not affect Exo activity. Thus, these structures provide a rationale for how A987G overcomes GCV-mediated chain termination.

Interestingly, the HCMV equivalent of the helical section (residues K833 to V838 in Fig. 7c), with which the yeast DNA polymerase δ residue corresponding to HCMV Pol A987 interacts, is the site of a deletion in an HCMV mutant (36). This deletion, like A987G, confers resistance to GCV and to the FDA-approved drug cidofovir (CDV), another delayed, nonobligate chain terminator that likely has a mechanism of termination similar to that of GCV (14, 37). We hypothesize that this mutant would, like A987G, exhibit increased rates of extension of GCV-containing primers.

Polymerase mutants from other systems containing mutations in the thumb subdomain (24, 28, 29, 38) have been reported to exhibit decreased polymerase activity relative to their WT counterparts, and these defects can be largely attributed to effects on primer binding. A987G Pol does exhibit a modest decrease in k_{cat} for dGTP incorporation, but the A987G substitution does not appear to meaningfully affect replicative fitness of the virus in cell culture (39). As this mutant has arisen in patients (18–20), it is also not highly crippled *in vivo*.

Our findings that WT HCMV Pol can readily extend RNA primers, which, to our knowledge, had not been previously reported, touch on a long-running literature regarding what enzyme extends RNA primers during herpesvirus DNA synthesis (25, 26, 27, 34, 40, 41). In particular, a thorough study from the Kuchta laboratory found that host DNA polymerase α-primase extended primers synthesized by the HSV-1 helicase-primase much more efficiently, i.e., much higher V_{max}/K_m values, largely due to a much lower K_m for dNTPs than the viral DNA polymerase (25). However, the Kuchta laboratory then elegantly demonstrated that viral proteins alone were sufficient for both leading- and lagging-strand synthesis on DNA minicircle templates and that DNA polymerase α-primase had no effect in this assay (34). These authors attributed the discrepancy in part to differences in template concentrations.

In the present study, we found much less marked differences in the extension of RNA and DNA primers by WT HSV-1 and HCMV Pols. Our studies were performed at high dNTP concentrations, where the Kuchta laboratory also found fairly similar rates of extension of RNA and DNA primers by HSV-1 DNA polymerase (25). As dNTP concentrations in HSV- and HCMV-infected cells are relatively high (16, 42), we think it likely that the viral DNA polymerases can efficiently extend RNA primers. During initiation of HCMV DNA synthesis, the viral polymerase might use transcripts generated by host RNA polymerase II that arise from or near the origin of replication (43, 44) as primers. During lagging strand synthesis, it would extend primers laid down by the viral helicase-primase. As the HCMV Pol A987G substitution increases the ability of the enzyme to utilize RNA primers, that might promote fitness of the mutant in the face of its reduced k_{cat} for dNTP incorporation.

Our results are relevant to other antiviral and anticancer nucleoside analogs that are nonobligate chain terminators. Some of them act in a delayed fashion, like GCV,

while others terminate DNA synthesis at the site of their incorporation. As mentioned above, the A987G substitution, but also several other alterations in the polymerase domain of HCMV Pol, confer resistance to CDV (37, 45). A more orally available prodrug of CDV, brincidofovir, is being developed to treat other DNA virus infections (46, 47). Enhanced extension of CDV-containing primers by A987G, and possibly other polymerase domain mutants, seems likely to account for its resistance to CDV. This hypothesis is currently under investigation. Similar mutations could emerge in other DNA viruses encoding family B polymerases. It is also conceivable that mutations enhancing elongation of drug-containing primers by host DNA polymerases affect the use of GCV in suicide therapies or contribute to resistance to nonobligate chain-terminating anticancer drugs, including ones with chain termination mechanisms that differ from that of GCV (e.g., gemcitabine [48]). In all these cases, as previously discussed (14), replicated DNA would contain internally incorporated nucleoside analogues that might increase mutation frequencies or strongly impair DNA synthesis when the replication machinery attempts to copy the DNA strands that contain drug. As a number of GCV^r Exo-deficient HCMV isolates and the A987G mutant are fit enough to replicate and cause disease in patients (13, 18–20), we hypothesize that DNA repair and/or recombination mechanisms may remove drug moieties from DNA to permit high rates of DNA synthesis without excessively high mutation frequencies.

We further speculate that mutations that enhance elongation of drug-containing primer strands contribute to resistance to approved and investigational nonobligate chain terminators of reverse transcription or RNA synthesis, such as certain anti-hepatitis B drugs (e.g., entecavir [49]), anti-human immunodeficiency virus drugs (e.g., islatravir [50]), anti-hepatitis C drugs (e.g., sofosbuvir [51]), and, of particular current interest, the anti-coronavirus drug remdesivir (52–56). In these cases, mechanisms other than exonuclease-mediated idling, such as slowed translocation, pyrophosphate-mediated excision, and/or polymerase backtracking, would be overcome by enhanced extension to overcome chain termination. Whether resistance would then require repair or recombination mechanisms to remove incorporated drug and whether such mechanisms would be available remain open questions.

MATERIALS AND METHODS

Construction of recombinant baculoviruses. Recombinant baculoviruses used to express WT Pol and A987G Pol were constructed using bacmids and methods described previously (14). Primers used for site-directed mutagenesis of plasmid pGST-WT Pol to generate the plasmid for glutathione *S*-transferase (GST)-tagged HCMV Pol mutant A987G were purchased from Integrated DNA Technologies: CTGGTGCGCAAGACGGGCTGCGAGT (forward) and CTTGACGAACTCGCAGCCCGTCTTGC (reverse).

Protein purification. WT Pol and A987G Pol, expressed as GST fusion proteins, were overexpressed in insect cells and purified using affinity chromatographic methods described previously (14). WT HSV-1 Pol was expressed as a 6×His-tagged protein and purified using affinity chromatography as described previously (33).

Oligonucleotides. Primer template T1 and 6-carboxyfluorescein (FAM)-labeled primer-template T5 and T6 were purchased from Integrated DNA Technologies. Primer-templates T2, T3, and T4 were synthesized by ChemGenes using GCV phosphoramidite prepared as described by Marshalko et al. (57). Sequences were confirmed in a synthesis report, and were validated by molecular mass determined by ESI mass spectrometry, and by step-wise incorporation of dNTPs by HCMV Pol. Purity was established by capillary electrophoresis.

Enzyme assays. Six different assays were performed: polymerase assays to measure apparent kinetic parameters (K_m, k_{cat}, and K_i), exonuclease assays, assays of full-length extension in the presence of GCV-TP, idling assays, single-nucleotide extension on GCV-containing primer-templates, and assays of full-length extension on FAM-labeled primer-templates using either RNA or DNA primers. Unless otherwise noted, all reactions with HCMV Pols were performed in 10-μl volumes at 37°C and contained 2.5 to 4 pmol of the indicated primer-template, either unlabeled or radiolabeled using [γ-^{32}P]ATP (PerkinElmer) and T4 polynucleotide kinase (New England Biolabs) or fluorescently labeled during synthesis as indicated; WT or mutant Pol, with or without a 2-fold molar excess of UL44ΔC290 (58) (kindly provided by Gloria Komazin-Meredith), as indicated; and polymerase buffer (50 mM Tris [pH 8.0], 1 mM dithiothreitol, 100 mM KCl, and 40 μg/ml bovine serum albumin). Reactions were initiated by adding $MgCl_2$ to 10 mM and, after incubation at 37°C for the times indicated, quenched using equal volumes of stopping buffer (0.05% bromophenol blue, 0.05% xylene cyanol, and 10 mM ethylenediaminetetraacetic acid [EDTA] in formamide) for polymerase and exonuclease reactions or 25 mM EDTA, 1% SDS, 5 mM dATP plus 5 mM dAMP for the idling assay, or 100 mM EDTA in 80% formamide for assays comparing extension of DNA or RNA primers on FAM-labeled primer-templates.

Apparent K_m and k_{cat} values for incorporation of dGTP and GCV-TP by WT Pol or the mutant Pol A987G were measured as described previously (14) using radiolabeled primer-template and conditions that meet the requirements for Michaelis-Menten kinetic analysis. The reactions were determined to be linear for 15 min using GCV-TP as the substrate and were stopped at 12 min, while those using dGTP as the substrate were linear for 10 min and stopped at 5 min. Kinetic parameters were measured using previously described methods (14, 28). Apparent K_i values were determined using a similar assay but with unlabeled primer template T1 and radiolabeled dGTP, whose incorporation was monitored using a filter-based method, as described previously (59).

Exonuclease assays were performed using polymerase buffer without any dNTPs added and 0.25 μM primer-template radiolabeled at its 5′ end, and, unless otherwise stated, 30 nM WT or mutant enzyme in the presence of a 2-fold molar excess of UL44ΔC290.

Full-length DNA extension by WT Pol and A987G Pol on primer-template T1 was assessed as described previously (14), with some modifications. Reactions were performed in polymerase assay buffer and contained 0.25 μM ^{32}P-labeled primer-template T1, each enzyme at 7.2 nM or 8.4 nM, a 2-fold molar excess of UL44ΔC290, 25 μM GCV-TP, and 25 μM dCTP/dATP/dTTP.

To assess single-nucleotide extension on various primer-templates, similar polymerase assays were performed, with details about the enzyme concentrations, radiolabeled primer templates, and the incorporated single nucleotides or nucleotide analogs provided in Table 2.

To assay full-length extension using a DNA primer on FAM-labeled primer-template T5 by WT Pol or A987G Pol, a 20-μl polymerase reaction was performed in the polymerase buffer described above, containing 20 nM enzyme, 40 nM primer-template T5, and 1 mM dATP/dTTP/dCTP/dGTP. A similar assay was applied to test the extension of an RNA primer on FAM-labeled primer-template T6 by WT Pol or A987G Pol, but each enzyme was preincubated with T6 at 37°C for 1 min before initiation of the reactions. A 2-fold molar excess of UL44ΔC290 was added to the same assay to test its effects on DNA or RNA primer extension by each enzyme. Assays of extension of DNA or RNA primers on FAM-labeled T5 or T6, respectively, using WT HSV-1 Pol were performed using the same conditions except that 25 mM HEPES (pH 7.5) and 25 mM NaCl were used instead of 50 mM Tris and 100 mM KCl, and reactions were initiated with 8 mM $MgCl_2$ (33).

For all of the above-described assays, except measurements of apparent K_is for GCV-TP, the products were separated on a 20% denaturing polyacrylamide gel, followed by quantification of radiolabeled products using a phosphorimager (Bio-Rad) or FAM-labeled products using an Amersham Typhoon 5 biomolecular imager (GE Healthcare) with detection at 520 nm following excitation at 495 nm.

Idling assays used 720 fmol each enzyme with UL44ΔC290, unlabeled primer-template T3, and 250 pmol dATP, including 10 μCi [α-^{32}P]dATP in the polymerase buffer based on previously reported methods (14, 60). The reactions were analyzed by thin-layer chromatography (TLC) on polyethyleneimine/cellulose (Sigma-Aldrich) in 0.1 M phosphate buffer (pH 7.0), followed by phosphorimager analysis.

Analysis of homologous polymerase structures. To find high-resolution structures with which to model the interaction of HCMV Pol with primer-template, we first searched the solved structures of family B DNA polymerase for those bound to primer-template. Of these, we then selected structures containing either of two DNA polymerases that allowed us to see the relevant parts of the ligands and were the closest homologs to HCMV Pol (61). These are yeast DNA polymerase δ bound to primer-template and incoming nucleotide (PDB entry 31AY) and RB69 bound to primer-template either with incoming nucleotide (PDB entry 1IG9) or without nucleotide in editing mode (PDB entry 1CLQ). The close homology of those structures to herpesvirus Pols was further validated by 5-sequence Clustal Omega simultaneous alignment and by the ability to superimpose the thumb domain of the HSV-1 Pol structure (15) in rigid-body superposition in a way that makes the topological correspondence obvious and permits assignment of residues that correspond to those in HCMV Pol. Figures were generated with PyMOL. The amino acid sequence alignment in Fig. 7a was generated using Clustal Omega.

SUPPLEMENTAL MATERIAL

Supplemental material is available online only.

FIG S1, TIF file, 0.1 MB.

FIG S2, TIF file, 0.9 MB.

FIG S3, TIF file, 0.1 MB.

FIG S4, TIF file, 0.1 MB.

FIG S5, TIF file, 0.5 MB.

FIG S6, TIF file, 2.6 MB.

ACKNOWLEDGMENTS

We thank Suresh Srivastava (ChemGenes) for his expertise in the synthesis of GCV-containing oligonucleotides, Gloria Komazin-Meredith for UL44, and Jean Pesola for advice on statistical analyses.

H.C., J.L.L., and D.M.C. designed research; H.C. and J.L.L. performed research; D.F. did structural modeling; H.C., J.L.L., D.F., J.H., and D.M.C. analyzed data; H.C., J.L.L., D.F., and D.M.C. wrote the paper.

This work was supported by the National Institutes of Health (grant number AI019838 to D.M.C. and J.M.H. and AI400048 to H.C.).

REFERENCES

1. Jordheim LP, Durantel D, Zoulim F, Dumontet C. 2013. Advances in the development of nucleoside and nucleotide analogues for cancer and viral diseases. Nat Rev Drug Discov 12:447–464. https://doi.org/10.1038/nrd4010.
2. Mocarski ES, Shenk T, Griffiths PD, Pass RF. 2013. Cytomegaloviruses, p 1960–2014. *In* Knipe DM, Howley PM (ed), Fields virology, 6th ed, vol 2. Lippincott Williams & Wilkins, Philadelphia, PA.
3. Coen DM, Richman DD. 2013. Antiviral agents, p 338–373. *In* Knipe DM, Howley PM (ed), Fields virology, 6th ed, vol 1. Lippincott Williams & Wilkins, Philadelphia, PA.
4. Castro MG, Lowenstein PR. 2013. The long and winding road—gene therapy for glioma. Nat Rev Neurol 9:609–610. https://doi.org/10.1038/nrneurol.2013.198.
5. Liang Q, Monetti C, Shutova MV, Neely EJ, Hacibekiroglu S, Yang H, Kim C, Zhang P, Li C, Nagy K, Mileikovsky M, Gyongy I, Sung H-K, Nagy A. 2018. Linking a cell-division gene and a suicide gene to define and improve cell therapy safety. Nature 563:701–704. https://doi.org/10.1038/s41586-018-0733-7.
6. Reid R, Mar E-C, Huang E-S, Topal MD. 1988. Insertion and extension of acyclic, dideoxy, and ara nucleotides by herpesviridae, human α and human β polymerases. A unique inhibition mechanism for 9–(1,3-dihydroxy-2-propoxymethyl)guanine triphosphate. J Biol Chem 263:3898–3904. https://doi.org/10.1016/S0021-9258(18)69010-6.
7. Mar E-C, Chiou H-F, Cheng Y-C, Huang E-S. 1985. Inhibition of cellular DNA polymerase α and human cytomegalovirus-induced DNA polymerase by the triphosphates of 9–(2-hydroxyethoxymethyl)guanine and 9–(1,3-dihydroxy-2-propoxymethyl)guanine. J Virol 53:776–780. https://doi.org/10.1128/JVI.53.3.776-780.1985.
8. Freitas VR, Smee DF, Chernow M, Boehme R, Matthews TR. 1985. Activity of 9-(1,3-dihydroxy-2-propoxymethyl)guanine compared with that of acyclovir against human, monkey, and rodent cytomegaloviruses. Antimicrob Agents Chemother 28:240–245. https://doi.org/10.1128/AAC.28.2.240.
9. Ilsley DD, Lee SH, Miller WH, Kuchta RD. 1995. Acyclic guanosine analogs inhibit DNA polymerase α, δ, and ε with very different potencies and have unique mechanisms of action. Biochemistry 34:2504–2510. https://doi.org/10.1021/bi00008a014.
10. Frank KB, Chiou J-F, Cheng Y-C. 1984. Interaction of herpes simplex virus-induced DNA polymerase with 9–(1,3-dihydroxy-2-propoxymethyl)guanine triphosphate. J Biol Chem 259:1566–1569. https://doi.org/10.1016/S0021-9258(17)43446-6.
11. Reardon JE. 1989. Herpes simplex virus type 1 and human DNA polymerase interactions with 2'-deoxyguanosine 5'-triphosphate analogues. Kinetics of incorporation into DNA and induction of inhibition. J Biol Chem 264:19039–19044. https://doi.org/10.1016/S0021-9258(19)47263-3.
12. Göhring K, Hamprecht K, Jahn G. 2015. Antiviral drug and multidrug resistance in cytomegalovirus infected SCT patients. Comput Struct Biotechnol J 13:153–159. https://doi.org/10.1016/j.csbj.2015.01.003.
13. Lurain NS, Chou S. 2010. Antiviral drug resistance of human cytomegalovirus. Clin Microbiol Rev 23:689–712. https://doi.org/10.1128/CMR.00009-10.
14. Chen H, Beardsley GP, Coen DM. 2014. Mechanism of ganciclovir-induced chain termination revealed by resistant viral polymerase mutants with reduced exonuclease activity. Proc Natl Acad Sci U S A 111:17462–17467. https://doi.org/10.1073/pnas.1405981111.
15. Liu S, Knafels JD, Chang JS, Waszak GA, Baldwin ET, Deibel MR, Thomsen DR, Homa FL, Wells PA, Tory MC, Poorman RA, Gao H, Qiu X, Seddon AP. 2006. Crystal structure of the herpes simplex virus 1 DNA polymerase. J Biol Chem 281:18193–18200. https://doi.org/10.1074/jbc.M602414200.
16. Biron KK, Fyfe JA, Stanat SC, Leslie LK, Sorrell JB, Lambe CU, Coen DM. 1986. A human cytomegalovirus mutant resistant to the nucleoside analog 9-([2-hydroxy-1-(hydroxymethyl)ethoxy]methyl)guanine (BWB759U) induces reduced levels of BW B759U triphosphate. Proc Natl Acad Sci U S A 83:8769–8773. https://doi.org/10.1073/pnas.83.22.8769.
17. Sullivan V, Biron KK, Talarico C, Stanat SC, Davis M, Pozzi LM, Coen DM. 1993. A point mutation in the human cytomegalovirus DNA polymerase gene confers resistance to ganciclovir and phosphonylmethoxyalkyl derivatives. Antimicrob Agents Chemother 37:19–25. https://doi.org/10.1128/aac.37.1.19.
18. Germi R, Mariette C, Alain S, Lupo J, Thiebaut A, Brion JP, Epaulard O, Raymond CS, Malvezzi P, Morand P. 2014. Success and failure of artesunate treatment in five transplant recipients with disease caused by drug-resistant cytomegalovirus. Antiviral Res 101:57–61. https://doi.org/10.1016/j.antiviral.2013.10.014.
19. Strasfeld L, Lee I, Tatarowicz W, Villano S, Chou S. 2010. Virologic characterization of multidrug-resistant cytomegalovirus infection in 2 transplant recipients treated with maribavir. J Infect Dis 202:104–108. https://doi.org/10.1086/653122.
20. Kaul DR, Stoelben S, Cober E, Ojo T, Sandusky E, Lischka P, Zimmermann H, Rubsamen-Schaeff H. 2011. First report of successful treament of multidrug-resistant cytomegalovirus disease with the novel anti-CMV compound AIC246. Am J Transplant 11:1079–1084. https://doi.org/10.1111/j.1600-6143.2011.03530.x.
21. Perera RL, Torella R, Klinge S, Kilkenny ML, Maman JD, Pellegrini L. 2013. Mechanism for priming DNA synthesis by yeast DNA polymerase α. Elife 2:e00482. https://doi.org/10.7554/eLife.00482.
22. Franklin MC, Wang J, Steitz TA. 2001. Structure of the replicating complex of a Pol α family DNA polymerase. Cell 105:657–667. https://doi.org/10.1016/S0092-8674(01)00367-1.
23. Swan MK, Johnson RE, Prakash L, Prakash S, Aggarwal AK. 2009. Structural basis of high-fidelity DNA synthesis by yeast DNA polymerase δ. Nat Struct Mol Biol 16:979–987. https://doi.org/10.1038/nsmb.1663.
24. Ganai RA, Bylund GO, Johansson E. 2015. Switching between polymerase and exonuclease sites in DNA polymerase ε. Nucleic Acids Res 43:932–942. https://doi.org/10.1093/nar/gku1353.
25. Cavanaugh NA, Kuchta RD. 2009. Initiation of new DNA strands by the herpes simplex virus-1 primase-helicase complex and either herpes DNA polymerase or human DNA polymerase alpha. J Biol Chem 284:1523–1532. https://doi.org/10.1074/jbc.M805476200.
26. Ramirez-Aguilar KA, Kuchta RD. 2004. Mechanism of primer synthesis by the herpes simplex virus I helicase-primase. Biochemistry 43:1754–1762. https://doi.org/10.1021/bi035519x.
27. Tsurumi T. 1991. Primer terminus recognition and highly processive replication by Epstein-Barr virus DNA polymerase. Biochem J 280:703–708. https://doi.org/10.1042/bj2800703.
28. Huang L, Ishii KK, Zuccola H, Gehring AM, Hwang CBC, Hogle J, Coen DM. 1999. The enzymological basis for resistance of herpesvirus DNA polymerase mutants to acyclovir: relationship to the structure of α-like DNA polymerases. Proc Natl Acad Sci U S A 96:447–452. https://doi.org/10.1073/pnas.96.2.447.
29. Blasco MA, Lázaro JM, Blanco L, Salas M. 1993. ø29 DNA polymerase active site. J Biol Chem 268:24106–24113.
30. Reardon JE, Spector T. 1989. Herpes simplex virus type 1 DNA polymerase. Mechanism of inhibition by acyclovir triphosphate. J Biol Chem 264:7405–7411. https://doi.org/10.1016/S0021-9258(18)83248-3.
31. Foti M, Marshalko S, Schurter E, Kumar S, Beardsley GP, Schweitzer B. 1997. Solution structure of a DNA decamer containing the antiviral drug ganciclovir: combined use of NMR, restrained molecular dynamics, and full relaxation matrix refinement. Biochemistry 36:5336–5345. https://doi.org/10.1021/bi962604e.
32. Dickerson RE. 1992. DNA structure from A to Z. Methods Enzymol 211:67–111. https://doi.org/10.1016/0076-6879(92)11007-6.
33. Lawler JL, Mukherjee P, Coen DM. 2017. Herpes simplex virus 1 DNA polymerase RNase H activity acts in a 3'-to-5' direction and is dependent on the 3'-to-5' exonuclease active site. J Virol 92:e01813-17. https://doi.org/10.1128/JVI.01813-17.
34. Stengel G, Kuchta RD. 2011. Coordinated leading and lagging strand DNA synthesis by using the herpes simplex virus 1 replication complex and

minicircle DNA template. J Virol 85:957–967. https://doi.org/10.1128/JVI.01688-10.
35. Shamoo Y, Steitz TA. 1999. Building a replisome from interacting pieces: sliding clamp complexed to a peptide from DNA polymerase and a polymerase editing complex. Cell 99:155–166. https://doi.org/10.1016/S0092-8674(00)81647-5.
36. Chou S, Miner RC, Drew WL. 2000. A deletion mutation in region V of the cytomegalovirus DNA polymerase sequence confers multidrug resistance. J Infect Dis 182:1765–1768. https://doi.org/10.1086/317618.
37. Xiong X, Smith JL, Chen MS. 1997. Effect of incorporation of cidofovir into DNA by human cytomegalovirus DNA polymerase on DNA elongation. Antimicrob Agents Chemother 41:594–599. https://doi.org/10.1128/AAC.41.3.594.
38. Kasiviswanathan R, Longley MJ, Chan SSL, Copeland WC. 2009. Disease mutations in the human mitochondrial DNA polymerase thumb subdomain impart severe defects in MtDNA replication. J Biol Chem 284:19501–19510. https://doi.org/10.1074/jbc.M109.011940.
39. Chou S. 2011. Phenotypic diversity of cytomegalovirus DNA polymerase gene variants observed after antiviral therapy. J Clin Virol 50:289–291. https://doi.org/10.1016/j.jcv.2011.01.004.
40. Wilcock D, Lane DP. 1991. Location of p53, retinoblastoma and host replication proteins at sites of viral replication in herpes-infected cells. Nature 349:429–431. https://doi.org/10.1038/349429a0.
41. Lee SS-K, Dong Q, Wang TS-F, Lehman IR. 1995. Interaction of herpes simplex virus 1 origin-binding protein with DNA polymerase α. Proc Natl Acad Sci U S A 92:7882–7886. https://doi.org/10.1073/pnas.92.17.7882.
42. Cheng Y-C, Goz B, Prusoff WH. 1975. Deoxyribonucleotide metabolism in herpes simplex virus infected HeLa cells. Biochim Biophys Acta 390:253–263. https://doi.org/10.1016/0005-2787(75)90346-9.
43. Pari GS. 2008. Nuts and bolts of human cytomegalovirus lytic DNA replication. Curr Top Microbiol Immunol 325:153–166. https://doi.org/10.1007/978-3-540-77349-8_9.
44. Spector DH. 2015. UL84-independent replication of human cytomegalovirus strains conferred by a single codon change in UL122. Virology 476:345–354. https://doi.org/10.1016/j.virol.2014.12.031.
45. Safrin S, Cherrington JM, Jaffe HS. 1997. Clinical uses of cidofovir. Rev Med Virol 7:145–156. https://doi.org/10.1002/(SICI)1099-1654(199709)7:3<145::AID-RMV196>3.0.CO;2-0.
46. Camargo JF, Morris MI, Abbo LM, Simkins J, Saneeymehri S, Alencar MC, Lekakis LJ, Komanduri KV. 2016. The use of brincidofovir for the treatment of mixed dsDNA viral infection. J Clin Virol 83:1–4. https://doi.org/10.1016/j.jcv.2016.07.021.
47. Crump R, Korom M, Buller RM, Parker S. 2017. Buccal viral DNA as a trigger for brincidofovir therapy in the mousepox model of smallpox. Antiviral Res 139:112–116. https://doi.org/10.1016/j.antiviral.2016.12.015.
48. Huang P, Chubb S, Hertel LW, Grindey GB, Plunkett W. 1991. Action of 2',2'-difluorodeoxycytidine on DNA synthesis. Cancer Res 51:6110–6117.
49. Seifer M, Hamatake RK, Colonno RJ, Standring DN. 1998. In vitro inhibition of hepadnavirus polymerases by the triphosphates of BMS-200475 and lobucavir. Antimicrob Agents Chemother 42:3200–3208. https://doi.org/10.1128/AAC.42.12.3200.
50. Michailidis E, Huber AD, Ryan EM, Ong YT, Leslie MD, Matzek KB, Singh K, Marchand B, Hagedorn AN, Kirby KA, Rohan LC, Kodama EN, Mitsuya H, Parniak MA, Sarafianos SG. 2014. 4'-Ethynyl-2-fluoro-2'-deoxyadenosine (EFdA) inhibits HIV-1 reverse transcriptase with multiple mechanisms. J Biol Chem 289:24533–24548. https://doi.org/10.1074/jbc.M114.562694.
51. Fung A, Jin Z, Dyatkina N, Wang G, Beigelman L, Deval J. 2014. Efficiency of incorporation and chain termination determines the inhibition potency of 2'-modified nucleotide analogs against hepatitis C virus polymerase. Antimicrob Agents Chemother 58:3636–3645. https://doi.org/10.1128/AAC.02666-14.
52. Agostini ML, Andres EL, Sims AC, Graham RL, Sheahan TP, Lu X, Smith EC, Case JB, Feng JY, Jordan R, Ray AS, Cihlar T, Siegel D, Mackman RL, Clarke MO, Baric RS, Denison MR. 2018. Coronavirus susceptibility to the antiviral remdesivir (GS-5734) is mediated by the viral polymerase and the proofreading exoribonuclease. mBio 9:e00221-18. https://doi.org/10.1128/mBio.00221-18.
53. Wang M, Cao R, Zhang L, Yang X, Liu J, Xu M, Shi Z, Hu Z, Zhong W, Xiao G. 2020. Remdesivir and chloroquine effectively inhibit the recently emerged novel coronavirus (2019-nCoV) in vitro. Cell Res 30:269–271. https://doi.org/10.1038/s41422-020-0282-0.
54. Sheahan TP, Sims AC, Graham RL, Menachery VD, Gralinski LE, Case JB, Leist SR, Pyrc K, Feng JY, Trantcheva I, Bannister R, Park Y, Babusis D, Clarke MO, Mackman RL, Spahn JE, Palmiotti CA, Siegel D, Ray AS, Cihlar T, Jordan R, Denison MR, Baric RS. 2017. Broad-spectrum antiviral GS-5734 inhibits both epidemic and zoonotic coronaviruses. Sci Transl Med 9:eaal3653. https://doi.org/10.1126/scitranslmed.aal3653.
55. Tchesnokov EP, Feng JY, Porter DP, Götte M. 2019. Mechanism of inhibition of Ebola virus RNA-dependent RNA polymerase by remdesivir. Viruses 11:326. https://doi.org/10.3390/v11040326.
56. Gordon C, Tchesnokov EP, Feng JY, Porter DP, Götte M. 2020. The antiviral compound remdesivir potently inhibits RNA-dependent RNA polymerase from Middle East respiratory syndrome coronavirus. J Biol Chem 295:4773–4779. https://doi.org/10.1074/jbc.AC120.013056.
57. Marshalko SJ, Schweitzer B, Beardsley GP. 1995. Chiral chemical synthesis of DNA containing (s)-9–(1,3-dihydroxy-2-propoxymethyl)guanine (DHPG) and effects on thermal stability, duplex structure, and thermodynamics of duplex formation. Biochemistry 34:9235–9248. https://doi.org/10.1021/bi00028a037.
58. Appleton BA, Loregian A, Filman DJ, Coen DM, Hogle JM. 2004. The cytomegalovirus DNA polymerase subunit UL44 forms a C clamp-shaped dimer. Mol Cell 15:233–244. https://doi.org/10.1016/j.molcel.2004.06.018.
59. Chen H, Li C, Zemlicka J, Gentry BG, Bowlin TL, Coen DM. 2016. Potency and stereoselectivity of cyclopropavir triphosphate action on human cytomegalovirus DNA polymerase. Antimicrob Agents Chemother 60:4176–4182. https://doi.org/10.1128/AAC.00449-16.
60. Garg P, Stith CM, Sabouri N, Johansson E, Burgers PM. 2004. Idling by DNA polymerase β maintains a ligatable nick during lagging-strand DNA replication. Genes Dev 18:2764–2773. https://doi.org/10.1101/gad.1252304.
61. Mönttinen HAM, Ravantti JJ, Stuart DI, Poranen MM. 2014. Automated structural comparisons clarify the phylogeny of the right-hand-shaped polymerases. Mol Biol Evol 31:2741–2752. https://doi.org/10.1093/molbev/msu219.